The University of Sydney

Department of Civil Engineering
Sydney NSW 2006
AUSTRALIA

http://www.civil.usyd.edu.au/

Centre for Advanced Structural Engineering

Design of Stainless Steel Roof Sections

Research Report No R851

Maura Lecce, BASc, MASc
Kim JR Rasmussen, MScEng, PhD

October 2005

The University of Sydney

Department of Civil Engineering
Centre for Advanced Structural Engineering
http://www.civil.usyd.edu.au/

Design of Stainless Steel Roof Sections

Research Report No R851

Maura Lecce, BASc, MASc
Kim Rasmussen, MScEng, PhD

October 2005

Abstract:

This report describes the influence of flange curling on cross-sectional properties and critical elastic buckling stresses of two wide-flanged roof sections (commercially available Monoclad and Megaclad). Results show that modified geometries due to flange curling can cause an increase of critical buckling stress ranging from 1.10 to 3.41 times that based on original geometries ignoring flange curling. Furthermore, the section modulus can be lowered from 6% to 16.9% due to flange curling deformations for the sections investigated. Flange curling was most significant for the more slender Megaclad section. The current proposed DSM design curve for the distortional buckling of stainless steel sections (Lecce and Rasmussen 2005a) and the Winter curve for local buckling are generally more conservative than the current North American Standard Appendix 1 (2004) DSM formulations. The design moment capacities alter due to flange curling and for distortional buckling there was an increase of up to 10.6% but a net decrease of up to 12.2% for local buckling. Given the current data, it would be prudent to ignore the effects of flange curling for distortional buckling but it would be necessary to consider them for local buckling.

Keywords:

Stainless steel, roof sheeting, local buckling, nonlinear flange curling, pure bending, distortional buckling, section modulus, yield moment, direct strength method.

Copyright Notice

Department of Civil Engineering, Research Report R851
Design of Stainless Steel Roof Sections

M.Lecce@civil.usyd.edu.au
K.Rasmussen@civil.usyd.edu.au

Published by:
Department of Civil Engineering
The University of Sydney
Sydney NSW 2006
AUSTRALIA

October 2005

This report and other Research Reports published by The Department of Civil Engineering are available on the Internet:

http://www.civil.usyd.edu.au

Table of Contents

List of Tables

List of Figures

Notation

I	=	moment of inertia
I_m	=	moment of inertia
M	=	bending moment
M_{cr}	=	critical bending moment
$M_{cr,d}$	=	critical bending moment for distortional buckling
$M_{cr,m}$	=	modified critical bending moment for distortional buckling accounting for
$M_{cr,l}$	=	critical bending moment for local buckling
$M_{cr,l}$	=	modified critical bending moment for local buckling
$M_{n,d}$	=	design moment capacity for distortional buckling
$M_{n,dm}$	=	modified design moment capacity for distortional buckling
$M_{n,l}$	=	design moment capacity for local buckling
$M_{n,lm}$	=	modified design moment capacity for local buckling
M_u	=	ultimate moment
$M_{u,avg}$	=	average ultimate moment
$M_{0.2}$	=	yield moment
$M_{0.2,m}$	=	modified yield moment
Z	=	section modulus
Z_f	=	section modulus to the extreme compression fibre
Z_{fm}	=	modified section modulus to the extreme compression fibre
Z_m	=	modified section modulus
f_{cr}	=	elastic critical buckling stress
$f_{cr,d}$	=	elastic distortional critical buckling stress
$f_{cr,d}$	=	modified elastic distortional critical buckling stress
$f_{cr,l}$	=	modified elastic local critical buckling stress
$f_{cr,l}$	=	elastic local critical buckling stress
f_y	=	yield stress
t	=	thickness
y	=	distance from neutral axis
y_m	=	distance from neutral axis
λ	=	slenderness
λ_d	=	distortional buckling slenderness
λ_{dm}	=	modified distortional buckling slenderness
λ_l	=	local buckling slenderness
λ_{lm}	=	modified local buckling slenderness
σ_y	=	yield stress
$\sigma_{0.01}$	=	0.01% proportionality stress
$\sigma_{0.2}$	=	0.2% proof stress
υ	=	Poisson's ratio = 0.3

1 Introduction

The purpose of this report is to assess the current direct strength design procedures for bending moment capacity of stainless steel roof sections. The flange curling of the wide-flange affects the distortional and local buckling behaviour and this report shows how the design is also affected. The experimental results of roof sections subject to pure bending was presented in Lecce and Rasmussen (Lecce and Rasmussen 2005b) and the theoretical evaluation of flange curling under changing geometric conditions presented in Lecce and Rasmussen (2005d).

Currently available literature on the design of steel decks subject to distortional or local buckling with the influence of flange curling is limited. Bernard et al. (1995) provides an evaluation of various design models and shows that the results were not consistent for various geometries and modes of failure. Although the interaction of local and distortional buckling was considered, the effects of flange curling were ignored. Davies and Chiu (2004) make a bold recommendation that the flange curling effects can be completely ignored in particular cases. From the literature available, there has been no prior attempt to theoretically model flange curling which causes changing geometric conditions and bring the results of this theoretical analysis into the assessment of current design equations.

This report explores the influence of flange curling on the cross-section properties and elastic critical buckling stress. The assessment of design equations for moment capacity ignoring and including effects of flange curling are presented. The Direct Strength Method is used as a basis for design

2 Elastic Buckling Analysis of Roof Sections

The ThinWall (Papangelis and Hancock 1995) finite strip elastic buckling analysis program was used to establish the cross-section gross properties and critical elastic buckling stresses of two wide-flanged sections named Monoclad and Megaclad. Two sets of analyses were considered: one where the cross-section is in its original form with perfect geometry; another where the geometry of the wide flange is adjusted for the flange curling effects (calculated at the average ultimate moment). The theoretical flange curling displacements of the wide flange were determined by the mathematical program Maple (Maplesoft 2003) (see Lecce and Rasmussen (2005d)) and the maximum center-pan displacements are given in Table 2.1. The flange curling displacements cause the wide flange to move closer to the neutral axis and hence the applied stress decreases towards the center of the flange. The applied stress distributions acting on the original cross-sections and the cross-sections modified to account for flange curling deformations are shown in Figures 2.1 and 2.2 for the Monoclad and Megaclad sections respectively. The flange curling deformations and associated stress distributions were calculated at the ultimate moment obtained in the tests.

Figures 2.3-2.6 show the critical buckling-stress versus half wavelength for the original and modified cross-sections for the distortional (wide flange in compression, WFC) and local buckling (wide flange in tension, WFT) of Monoclad sections and Megaclad sections, respectively. The minimum buckling stresses are highlighted by a diamond-shape data point. The gross cross-sectional properties and critical buckling stresses are given in Table 2.1. The properties based on a modified cross-section are given the subscript "*m*".

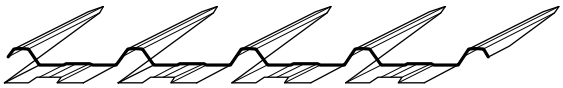

(a) Original cross-section

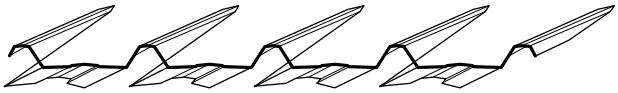

(b) Modified cross-section

Figure 2. 1. Monoclad Stress Distributions

(a) Original cross-section

(b) Modified section

Figure 2. 2 Megaclad Stress Distributions

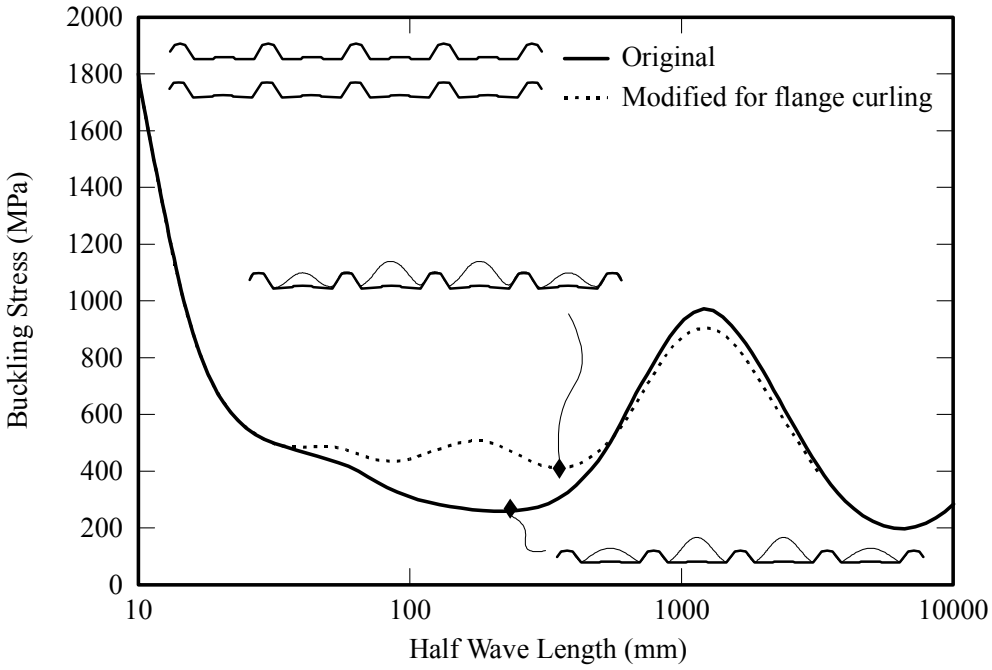

Figure 2. 3. Critical Buckling Stress: Mono_WFC

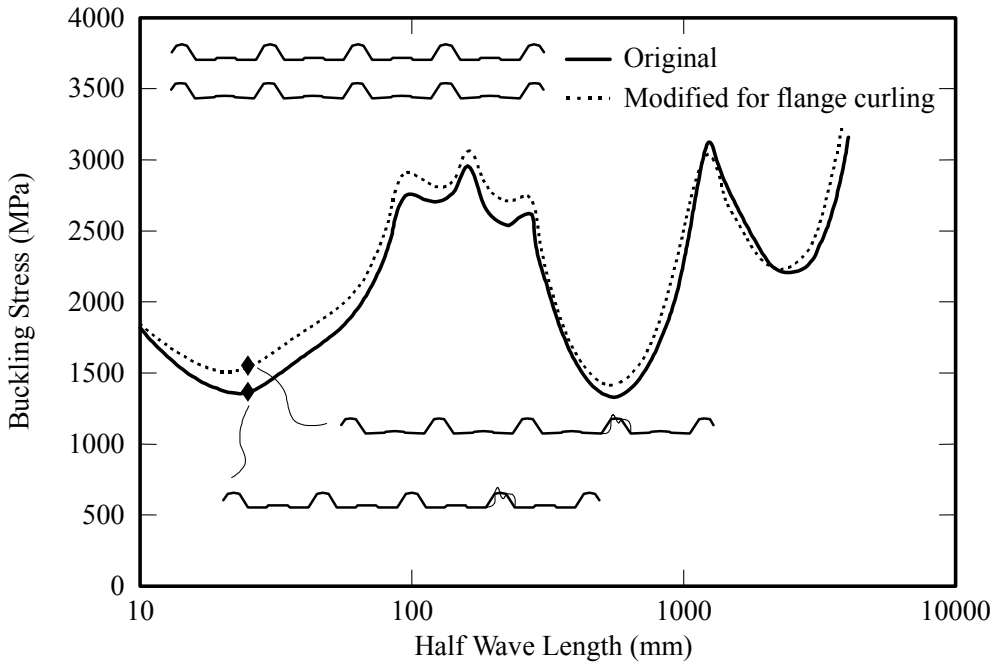

Figure 2. 4. Critical Buckling Stress: Mono_WFT

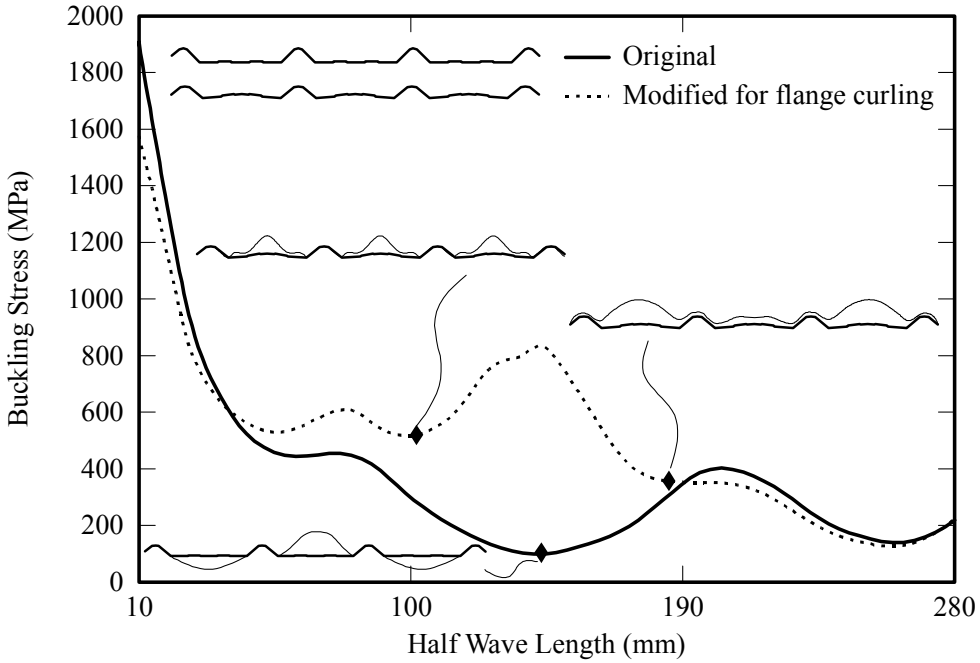

Figure 2. 5. Critical Buckling Stress: Mega_WFC

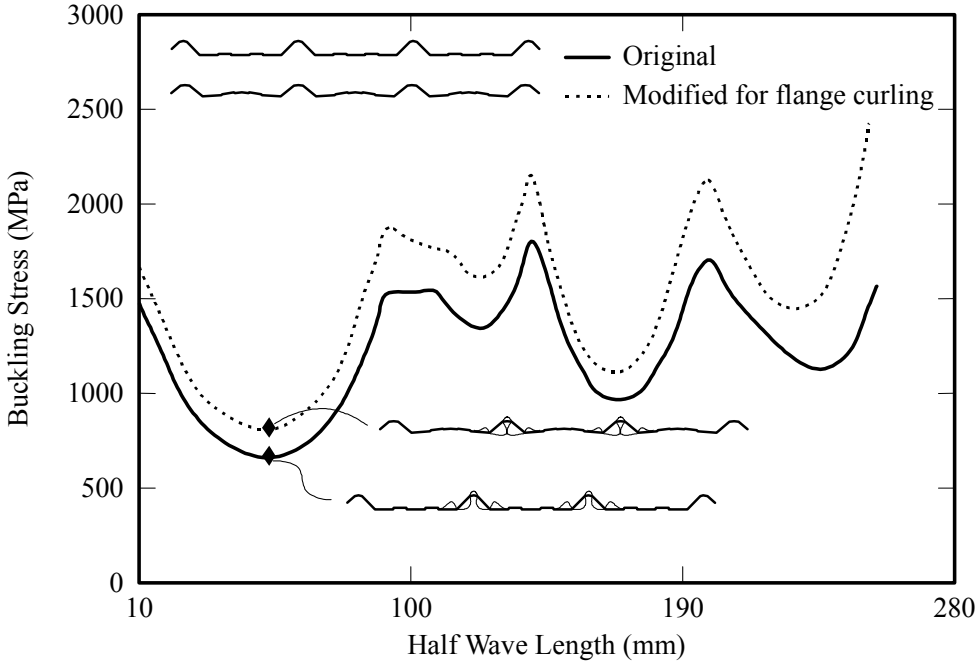

Figure 2. 6. Critical Buckling Stress: Mega_WFT

Evidently, because of flange curling deformations, the critical buckling stress increases. In the case of WFC (ie, distortional buckling critical) the half wavelength is also increased. These effects are the result of the cylindrical shape of the wide flange produced by flange curling which stiffens the cross-section against local and distortional modes of buckling.

As shown in Table 2.1 the increase in critical local buckling stress (WFT) due to flange curling ranges is 1.10 to 1.22 times that based on the original cross-section for Monoclad and Megaclad sections, respectively. The increase in critical distortional buckling stress (WFC) is 1.53 times for the Monoclad section and 3.41 times for the Megaclad section. Obviously, the impact of flange curling is much greater for the Megaclad section. It should be noted that the Megaclad section is significantly more slender than the Monoclad section and the corresponding wide-flange width to thickness ratios are 328 and 217. Although flange curling increases the critical buckling stress, the section modulus is reduced and this compromises the moment capacity. Table 2.1 shows that the section modulus is reduced by an average of 6% for the Monoclad section and 16.9% for the Megaclad section. These results obtained using ThinWall (Papangelis and Hancock 1995) are consistent with those presented in Lecce and Rasmussen (2005c), which describe the theoretical evaluations of flange curling deformations and changes to cross-section properties.

Table 2. 1. Original and Modified Geometric Properties and Critical Buckling Stresses

		Original Properties and Stresses (ThinWall)						Max. Disp. (Maple)	Modified Properties and Stresses (ThinWall)					Comparison	
Section	Orientation	$M_{u,avg}$	y	I	Z	Z_f	$f_{cr,d}$ or $f_{cr,l}$	u_m	y_m	I_m	Z_m	Z_{fm}	$f_{cr,dm}$ or $f_{cr,lm}$	Z_m/Z	$f_{cr,m}/f_{cr}$
		Nm	mm	mm^4	mm^3	mm^3	MPa	mm	mm	mm^4	mm^3	mm^3	MPa		
Mono	WFC	860	8.07	56980	2859	7062	275	1.70	8.61	52920	2729	6144	422	0.955	1.534
Mono	WFT	1150	8.07	56980	2859	2859	1371	3.11	9.06	49840	2632	2632	1509	0.921	1.101
Mega	WFC	694	6.47	43800	2243	6768	104	6.91	8.98	31830	1871	3543	355	0.834	3.413
Mega	WFT	740	6.47	43800	2243	2243	671	7.40	9.21	31210	1858	1858	824	0.828	1.228

The next Section investigates how these modified properties affect the design of roof sections in the direct strength method.

3 Direct Strength Method for Stainless Steel Roof Sections

The direct strength method provided in the latest North American Standard (NAS) Appendix 1 (2004) for cold-formed carbon steel is considered for the design of stainless steel roof sections. Furthermore, the well-known Winter curve and the proposed distortional buckling strength curve for stainless steel sections (Lecce and Rasmussen 2005a) are also considered in the design evaluations. The equations used in the DSM evaluations are as follows:

$$\lambda_d = \sqrt{\frac{M_y}{M_{cr,d}}} \qquad 1$$

$$M_{cr,d} = f_{cr,d} Z_f \qquad 2$$

$$\lambda_l = \sqrt{\frac{M_y}{M_{cr,l}}} \qquad 3$$

$$M_{cr,l} = f_{cr,l} Z_f \qquad 4$$

$$M_y = f_y Z \qquad 5$$

where, λ is slenderness, M_{cr} is the critical buckling moment, M_y is the yield moment, Z is the section modulus and Z_f is the section modulus calculated at the extreme compression fibre. The subscript "*d*" is given for distortional buckling and "*l*" is given for local buckling. (M_y and f_y are design moment and design yield stress, respectively but are replaced by $M_{0.2}$ and $\sigma_{0.2}$).

Distortional Buckling NAS Appendix 1(2004):

$$M_{n,d} = M_y \left[\frac{1}{\lambda_d} - \frac{0.22}{\lambda_d^{\,2}} \right] \le M_y \qquad 6$$

Local Buckling NAS Appendix 1 (2004):

$$M_{n,l} = M_y \left[\frac{1}{\lambda_l^{\,0.8}} - \frac{0.15}{\lambda_l^{\,1.6}} \right] \le M_y \qquad 7$$

Distortional Buckling (Lecce and Rasmussen 2005a):

$$M_{n,d} = M_y \left[\frac{0.90}{\lambda_d^{\,1.1}} - \frac{0.20}{\lambda_d^{\,2.2}} \right] \le M_y \qquad 8$$

Local Buckling Winter curve:

$$M_{n,l} = M_y \left[\frac{1}{\lambda_l} - \frac{0.22}{\lambda_l^{\,2}} \right] \le M_y \qquad 9$$

In Equations 6-9, M_n is the design moment capacity and the subscripts "*d*" and "*l*" represent distortional and local buckling, respectively.

The DSM evaluations using the NAS Appendix 1 (2004) (Equations 6 and 7) with the original cross sectional properties and critical stresses are given in Table 3.1. The critical buckling stresses, critical buckling moments and slenderness values are given in Table 3.1 for WFC (wide flange in compression) distortional buckling and for WFT (wide flange in tension) local buckling. The experimental ultimate moment (Lecce and Rasmussen 2005b) and yield moments based on the original section properties and critical buckling stresses are also given in Table 3.1.

Table 3. 1. DSM Evaluations Using Original Properties: NAS

		Test	Yield Moment			Section Modulus*	NAS DSM for Distortional Buckling					NAS DSM for Local Buckling				
Test ID	Orientation	M_u Nm	Z mm^3	$\sigma_{0.2}$ MPa	$M_{0.2}$ Nm	Z_f mm^3	$f_{cr,d}$ MPa	$M_{cr,d}$ Nm	λ_d	$M_{n,d}$ Nm	$M_u/M_{n,d}$	$f_{cr,l}$ MPa	$M_{cr,l}$ Nm	λ_l	$M_{n,l}$ Nm	$M_u/M_{n,l}$
MONO1	WFC	**878**	2859	346	989	7062	275	1941	0.71	959	**0.916**					
MONO2	WFC	**853**	2859	346	989	7062	275	1941	0.71	959	**0.890**			na		
MONO3	WFC	**845**	2859	346	989	7062	275	1941	0.71	959	**0.881**					
MONO7	WFT	**1179**	2859	346	989	2859			na			1371	3920	0.50	989	**1.192**
MONO8	WFT	**1121**	2859	346	989	2859						1371	3920	0.50	989	**1.133**
MEGA1	WFC	**679**	2243	388	870	6768	104	704	1.11	628	**1.082**					
MEGA2	WFC	**707**	2243	388	870	6768	104	704	1.11	628	**1.126**			na		
MEGA3	WFT	**726**	2243	388	870	2243			na			671	1506	0.76	870	**0.834**
MEGA4	WFT	**748**	2243	388	870	2243						671	1506	0.76	870	**0.859**
										mean	*0.979*				*mean*	*1.005*
										stdv	*0.1157*				*stdv*	*0.1841*
										cov	*0.1182*				*cov*	*0.1833*

* Section modulus calcuated at the extreme compression fibre

As shown in Table 3.1, the NAS (2004) provides reasonable moment capacities when the wide flange is in compression ($M_{n,d}$) for the more slender (λ_d=1.11) Megaclad section but is unconservative for the stockier Monoclad section (λ_d=0.71). The NAS (2004), based on cold-formed carbon steel, does not account for the stainless steel material nonlinearity which becomes more important for stockier sections (Lecce and Rasmussen 2005c) and could help explain why the Monoclad strength ratios ($M_u/M_{n,d}$) are less than unity. Considering the case where the wide flange is in tension, the predicted capacity for both Monoclad and Megaclad sections is governed by the yield moment (i.e., $M_{n,l} \leq M_y$). However, the ultimate moment for Megaclad sections is less than the yield moment which is partly due to flange curling effects. Flange curling has the effect of decreasing the section modulus (Z) and since $M_{0.2}=\sigma_{0.2}Z$ (or $M_y=f_yZ$) the moment at which yielding occurs also decreases. As shown in Table 2.1, the modified section modulus (Z_m) for the Megaclad section is 16.9% lower than Z due to flange curling effects. It has been shown that the Monoclad section is not as severely affected by flange curling and the mean $M_u/M_{n,l}$ is greater than unity. Overall, the NAS (2004) DSM using original cross-section properties is unconservative for the design of stainless steel roof sections in bending.

To account for stainless steel nonlinearity, the distortional buckling DSM curve developed in Lecce and Rasmussen (2005c) for ferritic alloys is adopted here (Equation 8) and the evaluations are given in Table 3.2. For local buckling, the Winter design curve given by Equation 9 is used. Evidently, the moment capacity predictions by the "Lecce & Rasmussen" DSM curve offers an improvement to those provided by the NAS (2004) and the mean test to predicted strength $M_u/M_{n,d}$ is 1.085 (c.f. mean $M_u/M_{n,d}$ =0.979 by NAS 2004). The Winter curve provides only a marginal difference in the strength predictions compared to the NAS 2004 and the mean $M_u/M_{n,l}$=1.034 and $M_u/M_{n,l}$=1.005, respectively.

Table 3. 2. DSM Evaluations Using Original Properties: Lecce & Rasmussen, Winter

		Test	Yield Moment			Section Modulus*	Lecce & Rasmussen DSM for Distortional Buckling					Winter for local buckling				
Test ID	Orientation	M_u **Nm**	Z mm^3	$\sigma_{0.2}$ MPa	$M_{0.2}$ Nm	Z_f mm^3	$f_{cr,d}$ MPa	$M_{cr,d}$ Nm	λ_d	$M_{n,d}$ Nm	$M_u/M_{n,d}$	$f_{cr,l}$ MPa	$M_{cr,l}$ Nm	λ_l	$M_{n,l}$ **Nm**	$M_u/M_{n,l}$
MONO1	WFC	**878**	2859	346	989	7062	275	1941	0.71	875	**1.004**					
MONO2	WFC	**853**	2859	346	989	7062	275	1941	0.71	875	**0.975**			na		
MONO3	WFC	**845**	2859	346	989	7062	275	1941	0.71	875	**0.966**					
MONO7	WFT	**1179**	2859	346	989	2859			na			1371	3920	0.50	989	**1.192**
MONO8	WFT	**1121**	2859	346	989	2859						1371	3920	0.50	989	**1.133**
MEGA1	WFC	**679**	2243	388	870	6768	104	704	1.11	559	**1.214**					
MEGA2	WFC	**707**	2243	388	870	6768	104	704	1.11	559	**1.264**			na		
MEGA3	WFT	**726**	2243	388	870	2243			na			671	1506	0.76	814	**0.892**
MEGA4	WFT	**748**	2243	388	870	2243						671	1506	0.76	814	**0.919**
										mean	*1.085*				*mean*	*1.034*
										stdv	*0.1428*				*stdv*	*0.1505*
										cov	*0.1317*				*cov*	*0.1455*

* Section modulus calcuated at the extreme compression fibre

Again, the discrepancy between the Monoclad and Megaclad results shown in Table 3.2 can be explained by the sections' sensitivity to flange curling.

To consider flange curling effects in the assessment of design guidelines, the modified properties and critical buckling stresses given in Table 2.1 (given subscript "m") are used in Equations 1-9. Table 3.3 shows the DSM evaluations according to the NAS Appendix 1 (2004) with the modified values and Table 3.4 shows those according to Lecce and Rasmussen (2005c) and Winter with the modified values.

Table 3. 3. DSM Evaluations Using Modified Properties: NAS

		Test				Section Modulus*	NAS DSM for Distortional Buckling					NAS DSM for Local Buckling				
Test ID	Orientation	M_u Nm	Z_m mm^3	$\sigma_{0.2}$ MPa	$M_{0.2,m}$ Nm	Z_{fm} mm^3	$f_{cr,dm}$ MPa	$M_{cr,dm}$ Nm	λ_{dm}	$M_{n,dm}$ Nm	$M_u/M_{n,dm}$	$f_{cr,lm}$ MPa	$M_{cr,lm}$ Nm	λ_{lm}	$M_{n,lm}$ Nm	$M_u/M_{n,lm}$
MONO1	WFC	**878**	2729	346	944	6144	422	2590	0.60	944	**0.930**					
MONO2	WFC	**853**	2729	346	944	6144	422	2590	0.60	944	**0.903**			na		
MONO3	WFC	**845**	2729	346	944	6144	422	2590	0.60	944	**0.895**					
MONO7	WFT	**1179**	2632	346	911	2632			na			1509	3972	0.48	911	**1.295**
MONO8	WFT	**1121**	2632	346	911	2632						1509	3972	0.48	911	**1.231**
MEGA1	WFC	**679**	1871	388	726	3543	355	1258	0.76	679	**1.000**					
MEGA2	WFC	**707**	1871	388	726	3543	355	1258	0.76	679	**1.041**			na		
MEGA3	WFT	**726**	1858	388	721	1858			na			824	1532	0.69	721	**1.007**
MEGA4	WFT	**748**	1858	388	721	1858						824	1532	0.69	721	**1.038**
* Section modulus calcuated at the extreme compression fibre										*mean*	*0.954*				*mean*	*1.143*
										stdv	*0.0641*				*stdv*	*0.1418*
										cov	*0.0672*				*cov*	*0.1241*

Evidently, accounting for the drop in section modulus and rise in critical buckling stress amounts to more consistent but not necessarily more conservative results. The coefficient of variations (COV) given in Table 3.3 (0.0672, 0.1241) is significantly less than those given in Table 3.1 (0.1182,0.1833). This implies that accounting for the effects of flange curling are important to obtain consistent results. Similarly, the COV results in Table 3.4 (0.0963, 0.1185) are much improved compared to those in Table 3.2 (0.1317,0.1455). The most drastic change in design capacities when flange curling is considered is with the Megaclad section. This is unsurprising since this section has been shown to have the greatest enhancement in distortional buckling stress and the greatest decrease in section modulus (see Table 2.1). Comparing Table 3.2 to Table 3.4, it is clear that the Megaclad $M_u/M_{n,d}$ ratio has dropped from an average of 1.239 (Table 3.2) to an average of 1.121 (Table 3.4). Therefore, the combination of increased critical buckling stress (and decreased slenderness) and reduced section modulus results in an average net increase in predicted capacity of 10.6%. The predicted local buckling capacity ($M_{n,l}$) is reduced by 12.2% if modified properties are considered, and the $M_u/M_{n,l}$ ratio goes from an average of 0.906 to 1.033 (compare Megaclad results in Tables 3.2 and 3.4).

For the Monoclad section, the $M_u/M_{n,l}$ ratio changes from an average of 1.163 to an average of 1.263 and so the design equations become increasingly conservative for this section when the changing geometry is accounted for. This is primarily because the section is fully effective (λ_l=0.50 and λ_{lm}=0.48), and hence parts of the cross-section are capable of reaching stresses higher than the 0.2% proof stress.

Overall, if distortional buckling is considered (or the wide flange is in compression) then flange curling produces a net positive effect which increases the predicted capacities and if otherwise is ignored then is conservative. However, if local buckling is considered (wide flange in tension) then the flange curling effects produce a net decrease in the predicted capacity and therefore more conservative results are obtained. Furthermore, the evaluations based on Lecce and Rasmussen (2005c) (Equation 8) for distortional buckling and Winter (Equation 9) for local buckling, provide more conservative results and would be suitable for the design of stainless steel sections.

Table 3. 4. DSM Evaluations Using Modified Properties: Lecce and Rasmussen, Winter

		Test				Section Modulus*	Lecce & Rasmussen DSM for Distortional Buckling					Winter for local buckling				
Test ID	Orientation	M_u **Nm**	Z_m mm^3	$\sigma_{0.2}$ MPa	$M_{0.2,m}$ Nm	Z_{fm} mm^3	$f_{cr,dm}$ MPa	$M_{cr,dm}$ Nm	λ_{dm}	$M_{n,dm}$ Nm	$M_u/M_{n,dm}$	$f_{cr,lm}$ MPa	$M_{cr,lm}$ Nm	λ_{lm}	$M_{n,lm}$ **Nm**	$M_u/M_{n,lm}$
MONO1	WFC	**878**	2729	346	944	6144	422	2590	0.60	907	**0.968**					
MONO2	WFC	**853**	2729	346	944	6144	422	2590	0.60	907	**0.940**			na		
MONO3	WFC	**845**	2729	346	944	6144	422	2590	0.60	907	**0.931**					
MONO7	WFT	**1179**	2632	346	911	2632			na			1509	3972	0.48	911	**1.295**
MONO8	WFT	**1121**	2632	346	911	2632						1509	3972	0.48	911	**1.231**
MEGA1	WFC	**679**	1871	388	726	3543	355	1258	0.76	618	**1.098**					
MEGA2	WFC	**707**	1871	388	726	3543	355	1258	0.76	618	**1.144**			na		
MEGA3	WFT	**726**	1858	388	721	1858			na			824	1531	0.69	714	**1.017**
MEGA4	WFT	**748**	1858	388	721	1858						824	1531	0.69	714	**1.048**
										mean	*1.016*				*mean*	*1.148*
										stdv	*0.0979*				*stdv*	*0.1360*
										cov	*0.0963*				*cov*	*0.1185*

* Section modulus calcuated at the extreme compression fibre

Given the present data, it would be prudent to ignore the effects of flange curling for the purpose of designing against distortional buckling but include them for the purpose of designing against local buckling. As shown in Lecce and Rasmussen (2005d), flange curling deformations can be determined sufficiently accurately from an analysis based on the original cross-section geometry, (while the applied stress distribution cannot). A suitable, accurate design procedure for sections with the wide flange in tension is thus:

- Determine the design moment ($M_{n,l}$) on the basis of the original cross-section geometry using the Direct Strength Method
- Determine the flange curling deformations at this moment
- Modify the cross-section geometry to account for flange curling deformations
- Determine the design moment capacity for the modified cross-section using the Direct Strength Method

It is recognized that these recommendations are based on relatively few results and more data are required to establish the geometric limits for which flange curling becomes significant enough to justify consideration in design. For the assessment presented here, it is reasonable to ignore the effects of flange curling for the Monoclad section whether designing against local or distortional buckling, but the same simplification would not be practical for the Megaclad section. Finally, there is now an understanding of the flange-curling phenomenon, how it affects the distortional and local buckling behaviour and in turn its impact on the design of stainless steel roof sections.

4 Conclusions

The results of elastic buckling analysis of wide-flange roof sections both ignoring and including flange curling deformations have been presented. Overall, an increase in buckling stress results when flange curling deformations are included. The influence of flange curling is greater for the Megaclad section, with a wide flange to thickness ratio of 328, and there is an increase in distortional buckling stress of 241% times that based on an analysis without flange curling considered. The increase in local buckling stress was 22% due to flange curling for the Megaclad section. By the same phenomenon, the section modulus is decreased by 6% for the Monoclad section and 16.9% for the Megaclad section. The assessment of design equations for the distortional and local buckling of roof sections subject to bending shows significant scatter in the results if flange curling effects are ignored. The predicted capacity for the Megaclad section is too conservative for distortional buckling but is significantly unconservative for local buckling. Including the effects of flange curling in the design show a marked decrease in the scatter of results showing the importance of

capturing the geometric changes in the wide flange. Given the limited experimental data, it is prudent to recommend that flange curling should be ignored in the design against distortional buckling but that it should be included for the design of local buckling. The proposed DSM for the distortional buckling of stainless steel sections (Lecce and Rasmussen, 2005a) and the Winter curve for local buckling (with modified properties and stresses to account for flange curling) are more suitable for predicting the moment capacities than the current NAS Appendix 1 (2004) for cold-formed carbon steel. An accurate calculation of flange curling deformations can be found in Lecce and Rasmussen (2005d).

5 References

Bernard, E. S., Bridge, R. Q., and Hancock, G. J. (1995). "Tests of Profiled Steel Decks with Flat-Hat Stiffeners." *Journal of Structural Engineering*, 121(8), 1175-1182.

Davies, J. M., and Chiu, R. (2004). "Flange Curling in Slender Sections." *Proc., 4th Specialty Conference on Cold-Formed Steel Structures.*, IOP Publishing Ltd.

Lecce, M., and Rasmussen, K. J. R. (2005a). "Distortional Buckling of Cold-Formed Stainless Steel Sections: Finite Element Modeling and Design." *Journal of Structural Engineering*, in press.

Lecce, M., and Rasmussen, K. J. R. (2005b). "Experimental Investigation of Stainless Steel Roof Sections in Pure Bending." Research Report No.847, Department of Civil Engineering, University of Sydney, Sydney.

Lecce, M., and Rasmussen, K. J. R. (2005c). "Finite Element Modelling and Design of Cold-Formed Stainless Steel Sections." Research Report No. 845, Department of Civil Engineering, University of Sydney, Sydney.

Lecce, M., and Rasmussen, K. J. R. (2005d). "Nonlinear Flange Curling of Wide-flange Sections." Research Report No. 850, Department of Civil Engineering, University of Sydney, Sydney.

Maplesoft. (2003). "Maple 9.03." Waterloo Maple Inc.

NAS. (2004). "Appendix 1 Design of Cold-Formed Steel Structural Members with the Direct Strength Method." American Iron and Steel Institute, Washington, D.C.

Papangelis, J. P., and Hancock, G. J. (1995). "Computer Analysis of Thin-Walled Structural Members." *Computers & Structures*, 56(1), 157-176.